View metadata, citation and similar papers at core.ac.uk
brought to you by CORE
provided by Minds@University of Wisconsin

Proceedings of the 8th International Conference on MicroManufacturing
University of Victoria, Victoria, BC, Canada, March 25-28, 2013

Influence of Process Parameters on the Deformation of Copper Foils in Flexible-Pad Laser Shock Forming

ICOMM 2013 No.48

Balasubramanian Nagarajan [1,2,a], Sylvie Castagne [1,2,b], and Zhongke Wang [1,3]

[1] SIMTech-NTU Joint Laboratory (Precision Machining), Nanyang Technological University, 50 Nanyang Avenue, Singapore 639798
[2] School of Mechanical and Aerospace Engineering, Nanyang Technological University, 50 Nanyang Avenue, Singapore 639798
balasubr2@e.ntu.edu.sg [a,*], scastagne@ntu.edu.sg [b]
[3] Machining Technology Group, Singapore Institute of Manufacturing Technology, Singapore 638075
zkwang@SIMTech.a-star.edu.sg

Key Words: Microforming, laser shock forming, laser-induced shock pressure, confinement layer, ablative overlay

ABSTRACT

This paper investigates a new microforming technique, Flexible-Pad Laser Shock Forming (FPLSF), to produce microfeatures on metallic foils without rigid punches and dies. FPLSF uses the laser-induced shock pressure and a flexible-pad to plastically deform metal foils into hemispherical microcraters. In order to understand the deformation characteristics of metal foils in FPLSF, it is necessary to analyze the influence of process parameters on the foil deformation. In this paper, the effects of parameters such as the flexible-pad thickness, confinement layer medium, confinement layer thickness and the number of laser pulses on the depth, diameter and shape of the craters formed on copper foils were investigated. It is found that the flexible-pad thickness should be greater than its threshold value to maximize the deformation of foils. By comparing two different confinement media, namely water and glass, it is observed that hemispherical craters were formed on the copper foils at different laser fluence values tested when using water as the confinement; whereas shockwave ripples were formed on the copper foil at higher laser fluence while using the glass confinement. Using water as confinement medium, an increase in confinement thickness from 4 mm to 7 mm resulted in 48% increase of the crater depth at 7.3 J/cm^2. However, at 13.6 J/cm^2, reduction in crater depth was observed for thickness greater than 6 mm after an initial increasing trend. Regarding the number of pulses, it is found that increasing the number of pulses from 1 to 3 resulted only in a small increase (less than 1%) in crater depth at 7.3 J/cm^2 and 13.6 J/cm^2 laser fluence whereas 19.3% increase in depth was observed at larger laser fluence (20.9 J/cm^2). It is also observed that the optimum number of pulses to achieve maximum deformation is varying with the laser fluence.

INTRODUCTION

Laser shock forming (LSF) is a micromanufacturing technique which uses laser-induced shock pressure and mold patterns to form 3D microstructures on metallic sheets. A new microforming technique, Flexible-Pad Laser Shock Forming (FPLSF) which induces plastic deformation on metallic foils using non-contact laser-induced shock pressure and a flexible polymer backing pad, has been developed recently [1]. A significant advantage of this high strain-rate FPLSF process is that it employs no rigid mold patterns or punches to plastically deform the foils. FPLSF provides considerable improvement in microforming in terms of process cycle time and cost as it eliminates the complex mold fabrication as well as the alignment of the mold and laser beam to produce microfeatures. FPLSF could be applicable to electronics, optics, and biomedical components due to its ability to produce complex 3D features on metallic foils.

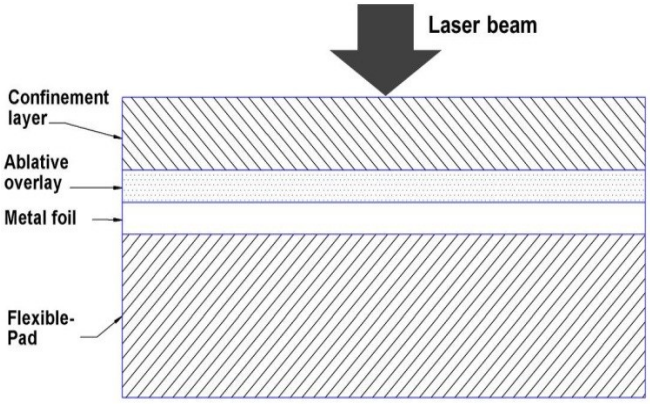

Fig. 1. Schematic of Flexible-Pad Laser Shock Forming [1]

The schematic of FPLSF is shown in Fig. 1. The working principle of FPLSF is as follows: the foil is placed over the flexible rubber pad which follows a hyperelastic material behavior. A high-energy pulsed laser beam passes through a transparent confinement layer and irradiates the ablative overlay which is placed on top of the metal foil. The ablative overlay is vaporized instantaneously and generates high pressure plasma. The produced plasma expands in the confined space and induces a shockwave towards the metal foil. Once the shockwave pressure exceeds the dynamic yield strength of the metal, plastic deformation of the foil occurs. Flexible-pad undergoes hyperelastic deformation along with the deformation of metal. It then retracts to its original state once the loading is completed. FPLSF is highly flexible due to its flexible-pad arrangement, in which the same pad can be

used to produce various shapes by changing the process parameters.

FPLSF has various process components such as confinement layer, ablative overlay, flexible-pad and the laser system. However, the influence of several process parameters on the plastic deformation of metallic foils is yet to be investigated. Laser pulse energy has been a significant process parameter in the processes using laser-induced shockwaves as it influences the ablation of overlay/coating and hence the amplitude of induced-shock pressure [2, 3]. The deformation depth of metal sheets increased with an increase in number of pulses in laser deep drawing whereas the sheets fractured after reaching a deformation threshold [2]. In order to avoid the bounce-off effect and the failure of sheets during forming, the total laser energy was evenly distributed between the pulses. By using this technique, it was observed that the deformation depth increased until a threshold after which it reduced [4]. It is understood that there is an optimum level of number of pulses to achieve the maximum deformation in laser shock forming process.

Confinement layer has been used to restrict the plasma diffusion and increase the peak pressure. Materials such as K9 glass, perspex, quartz glass, silicon rubber, and Pb glass were used as the confinement medium [5]. As the induced shock pressure depends upon the shock impedance of the confinement material [6], difference in shock pressure for different confinement medium was observed. Using water as the confinement increased the plasma pressure by ten times compared to the direct ablation mode and increased the bending angle in laser forming of the stainless steel sheets [7]. The confinement layer also increases the shock pressure duration [6]. However, at higher laser intensity the dielectric breakdown of confinement materials such as glass and water saturates the shock pressure duration and the peak pressure [6, 8].

A confinement thickness smaller than a critical value(e_m) [$e_m = 0.5\tau D$ where τ is the laser pulse width and D is the shock velocity] will reduce the peak pressure due to the reflected shockwave from the free surface [9]. Also, the peak plasma pressure was found to be increasing along with an increase in confinement thickness until a threshold of thickness was reached [10]. Thus, the thickness of the confinement layer is also found to be a significant process parameter in laser shock forming.

Ablative overlay is a sacrificial component in conventional laser shock forming and FPLSF that is vaporized due to high temperature and pressure of laser irradiation. Graphite, thin aluminum foils and black paint have been used as the ablative overlay material [11, 12].

In FPLSF, a flexible-pad supports the metal foil and undergoes hyperelastic deformation during the shock loading. For analysis purpose, the FPLSF process can be related to rubber pad forming, which uses metal punches and rubber dies to deform the sheets. In rubber pad forming, materials such as natural rubber, silicone rubber and polyurethane rubber are commonly used as the rubber pad [13, 14]. It is found that silicone rubber requires lower punch load and is suitable when the number of loading cycles are less whereas polyurethane rubber is appropriate for a large number of cycles [13]. It is found that there exists an optimum pad thickness to maximize the deformation depth as the depth saturates once the pad thickness reaches a certain threshold [15]. The thickness of rubber pad in this process is prescribed to be at least 2 or 3 times larger than the forming depth [16, 17]. As FPLSF is a high-strain-rate process and also involves micro-mesoscale deformation compared to the quasi-static macroscale rubber pad forming, the loading and deformation behaviors are different. Therefore, the influence of pad thickness on the deformation in FPLSF needs to be understood.

It is found from processes involving laser-induced shock pressure that the laser energy, number of pulses, confinement medium and its thickness, affect the plasma-induced shock pressure and the plastic deformation significantly. Therefore, it is crucial to investigate these parameters in case of FPLSF to understand and optimize the process. In this paper, parameters such as the flexible-pad thickness, number of laser pulses, confinement layer medium and its thickness are investigated against the depth and diameter of the craters formed by FPLSF.

MATERIALS AND METHODS

Copper foils (99.9%) of 25 μm thickness were used as the workpiece. A Nd:YAG (Q-switched) laser with the following parameters was used for the irradiation: wavelength = 1064 nm, pulse duration = 38 ns, maximum pulse energy = 75 mJ at 6 KHz, beam size = 600 μm x 600 μm. Silicone rubber was chosen as the flexible-pad for all experiments due to its better loading capacity and the number of cycles is low in this experiment. Fused silica glass (6 mm thick) and deionized water were used as the confinement layer. Black paint and aluminum foil were tested initially for ablative overlay. It was found that black paint as the overlay has limitations in terms of difficulty in removal after the process, spallation of paint to the non-irradiated zone, and producing uniform thickness. So, aluminum foil (15 μm thickness) was used as the ablative overlay as it has a smaller vaporization threshold and can be easily removed after FPLSF. A small layer of vacuum grease was applied between the ablative overlay and the copper foil for tight sealing.

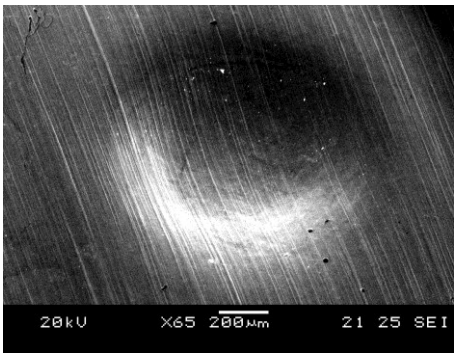

Fig. 2. Top surface of the crater formed on copper foil using FPLSF at 7.3 J/cm^2 laser fluence

A surface profiler (Taylor Hobson Talyscan 150) was used to observe the crater surface topographies and measure the crater dimensions. Crater depth (d) and projected crater di-

ameter (D_c) were measured using a stylus probe (2 μm radius diamond tip) through scanning the top surface of the formed crater. Optical microscope and Scanning Electron Microscope were used to investigate the surface quality of the formed craters and the ablation behavior of aluminum foil overlay. Fig. 2 shows the SEM image of the top surface of the formed crater at 7.3 J/cm^2 fluence using water confinement (4.2 mm thickness). All experiments in this paper were repeated three times and the average value of crater dimensions is plotted.

RESULTS AND DISCUSSIONS

A. EFFECT OF FLEXIBLE-PAD THICKNESS

The pad thickness was examined at the following conditions: laser fluence = 13.6 J/cm^2; number of pulses = 1; confinement layer = water; confinement thickness = 4.2 mm. The flexible-pad thickness was tested at three levels = 0.3 mm, 0.6 mm, and 0.9 mm.

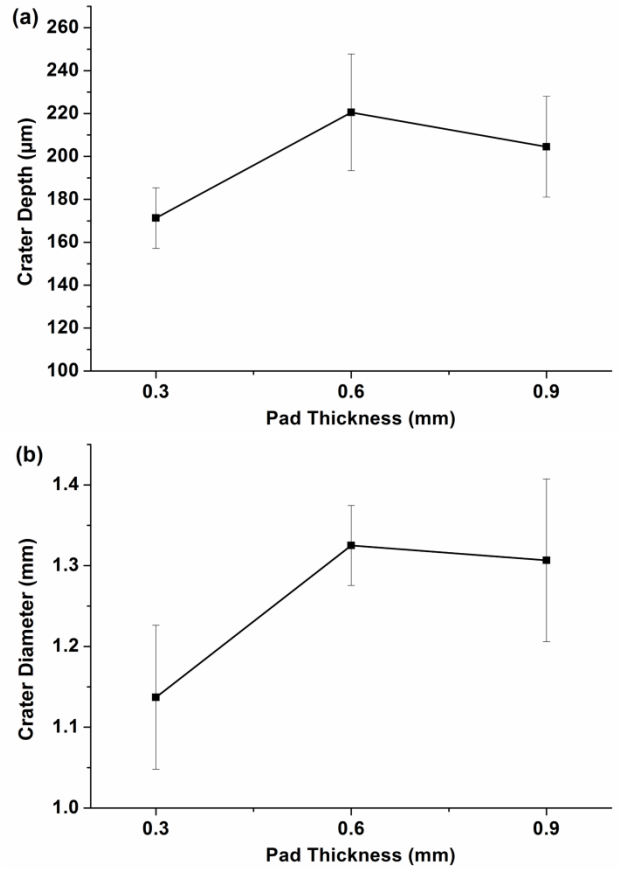

Fig. 3. Comparison of crater dimensions with flexible-pad thickness at 13.6 J/cm^2 laser fluence in FPLSF (a) Crater Depth (b) Crater diameter

The effect of pad thickness on depth and diameter of the formed crater is shown in Fig.3. It can be observed that the crater depth increased sharply for an increase in pad thickness from 0.3 mm to 0.6 mm. When the thickness is increased further to 0.9 mm, the crater depth slightly decreased. However, considering the standard deviation it can be understood that the crater depth decreases or attains saturation after reaching 0.6 mm. Similarly, increase crater diameter was observed when the pad thickness increased from 0.3 mm to 0.6 mm whereas the diameter saturates after 0.6 mm.

The smaller crater depth and diameter with lesser pad thickness could be attributed to the following factors:

- The rubber pad is compressed when the foil deforms due to the shockwave propagation. The pad cannot be compressed further once it reaches its maximum limit. Then, the pad will induce a counter pressure towards the foil which acts in the direction opposite to the shock pressure. This counter pressure will restrict the deformation of foil which will lead to the reduction in crater depth. The amplitude of the back pressure depends upon the pad thickness and the mechanical properties of the pad such as stiffness.
- When the pad thickness is small, elastic waves propagating in the rubber will induce a rarefaction wave when the plastic wave is still propagating in the metal foil. This rarefaction wave could lead to the reduction in amplitude of the plastic wave and hence the reduction in the deformation of the foil.

In FPLSF, the shock pressure propagating from the foil top surface will be the same irrespective of the flexible-pad thickness. However, it is interesting to observe with FPLSF that the flexible-pad which is elastically deforming along with the plastically deforming copper foil influences the stress distribution along the foil and the deformation characteristics. This behavior is different from laser shock forming processes where the deformation of metal foils depends on the shock pressure induced by the laser ablation of overlay material. Though the threshold pad thickness was found to be 0.6 mm from Fig. 3, pad thickness of 0.9 mm was used in the following experiments to comply with having pad thickness three times greater than the maximum crater depth observed [17] as the crater depth increases at higher laser fluence.

B. EFFECT OF CONFINEMENT MEDIUM

Fused silica glass and water confinements were investigated at three different laser fluence values (7.3 J/cm^2, 13.6 J/cm^2 and 20.9 J/cm^2) at single pulse irradiation. The thicknesses of water confinement and pad were 4 mm and 0.9 mm respectively.

The depth and diameter of the craters formed at different laser fluence for water and glass confinements are shown in Fig. 4. It can be observed that the depth and diameter of the crater increased with the increase in laser fluence for both the water and glass confinements. The depth of the craters formed by FPLSF strongly depends upon the laser-induced shock pressure [1]. As the shock pressure is proportional to the laser intensity, the crater depth increased with increase in laser fluence for both water and glass confinements. The diameter of the crater is proportional to the beam size. The increase in crater diameter with fluence is attributed to the change in ablation behavior of aluminum foil with fluence. Figure 5 compares the ablation behavior of aluminum foil overlay for water and glass confinements at different laser fluence. As the same beam with uniform spatial intensity profile was used in this experiment, the variation in crater diameter for the increase in laser fluence has been small as compared to the change in crater depth.

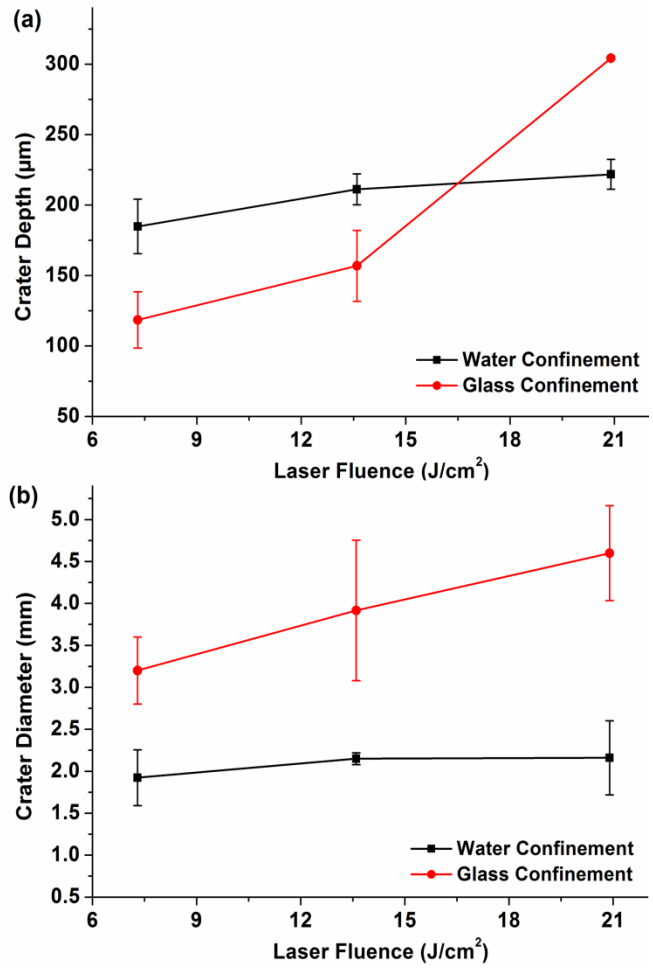

Fig. 4. Comparison of dimensions of craters formed by FPLSF using water and glass confinements (a) Crater Depth (b) Crater diameter

It is observed from Fig. 4a that the crater depth with water confinement was higher than that of glass confinement at 7.3 J/cm^2 and 13.6 J/cm^2 laser fluence. But, higher deformation depth was expected with glass confinement due to the following factors:

- According to Fabbro's shock pressure model, the induced shock pressure is directly proportional to the shock impedance of the target and confinement materials [6]. As the shock impedance of glass is greater than the shock impedance of water, the induced-shock pressure will be higher with glass and hence a deeper crater is expected.
- Also, as the transmittance of fused silica glass at 1064 nm wavelength (93.9%) is higher than that of water (80.3%), the laser energy at the ablative overlay surface will be higher with glass confinement.

The higher deformation depth with water confinement is attributed to the following behaviors:

– Due to the large irradiation energy with glass, the aluminum foil overlay was completely ablated as shown in Fig. 5a and exposed the copper foil to laser beam. This causes the vaporization of copper foil top surface (as shown in Fig. 6a and Fig. 6b) which results in the reduction of induced shock pressure and hence the reduction in the crater depth.

– (With glass confinement, the accurate sealing between foil and glass is not maintained throughout the foil forming duration as the confinement breaks off once the foil starts deforming. In case of water, perfect confinement exists during the entire laser irradiation and the foil deformation. This behavior can be seen from Fig. 4b, where larger crater diameter was observed for glass confinement at all laser fluence due to the free expansion of plasma in the radial direction. It can also be observed from Fig. 5 that the ablated area of aluminum foil increases with the laser fluence with glass confinement whereas the ablated area of aluminum has been uniform with water confinement.

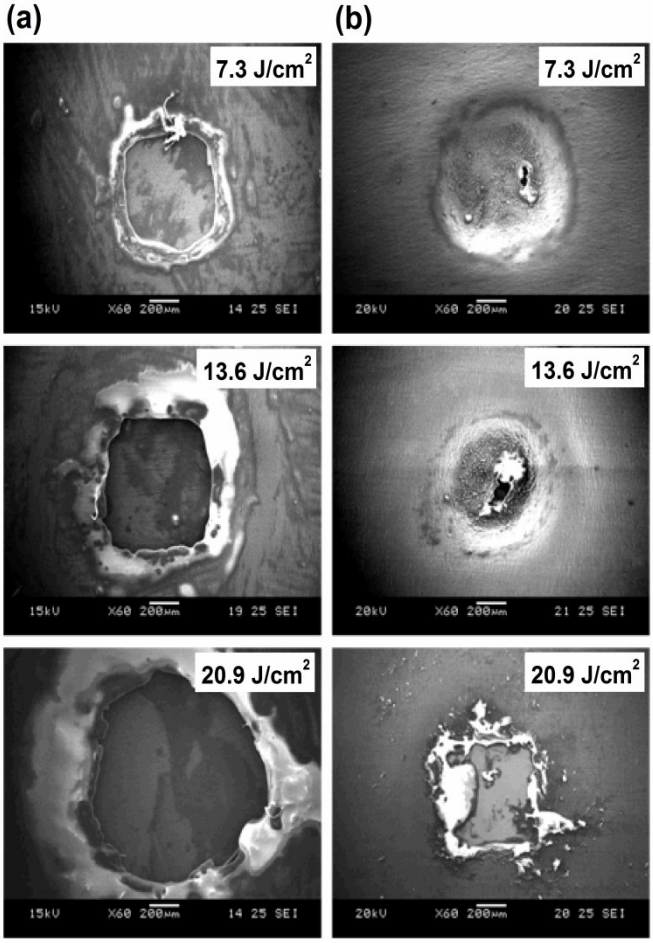

Fig. 5. Ablation behavior of aluminum foil overlay at different laser fluence in FPLSF with (a) Glass confinement (b) Water confinement

The surface topography of craters at different laser fluence is shown in Fig. 7. It can be seen that the hemispherical-shaped craters were formed at all laser fluence levels tested when using water confinement. In case of glass confinement, though the lesser laser fluence (7.3 J/cm^2 and 13.6 J/cm^2) produced hemispherical craters, shockwave ripples were formed on the copper foils at 20.9 J/cm^2 fluence as shown in Fig. 7a. This formation of shockwave structures on the copper foil could be attributed to the wave guidance of the shockwave by the glass at higher laser fluence. This behavior is also responsible for the higher crater depth with glass confinement at 20.9 J/cm^2 (Fig. 4a) and significant increase in crater diameter as shown in Fig. 4b. Damage of the fused silica glass

surface was also observed at 20.9 J/cm^2 fluence (Fig. 6c). It is noted from Fig. 6 that the top surface of the crater was ablated at 13.6 J/cm^2 (Fig. 6a) and 20.9 J/cm^2 (Fig. 6b) with glass confinement whereas damage-free crater surface was produced with water confinement even at the maximum laser fluence of 20.9 J/cm^2 (Fig. 6d).

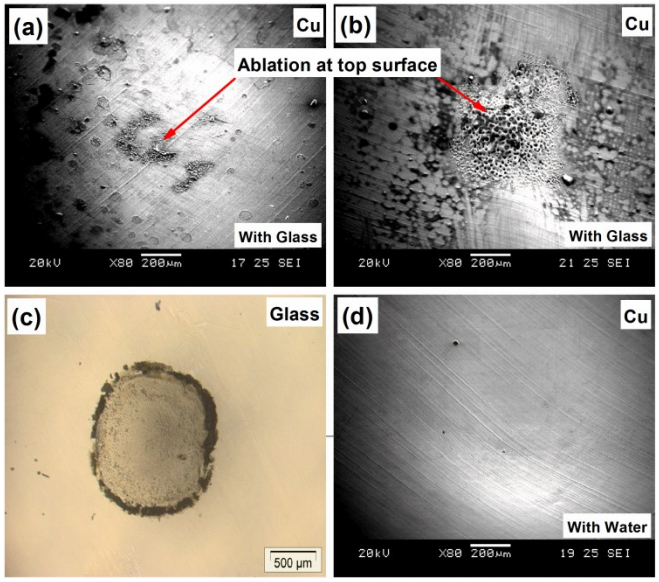

Fig. 6. Surface integrity of copper top surface with glass and water confinements in FPLSF (a) Ablation of copper surface at 13.6 J/cm^2 laser fluence with glass (b) Ablation of copper surface at 20.9 J/cm^2 laser fluence with glass (c) Damage of fused silica glass at 20.9 J/cm^2 (d) Copper top surface at 20.9 J/cm^2 with water confinement

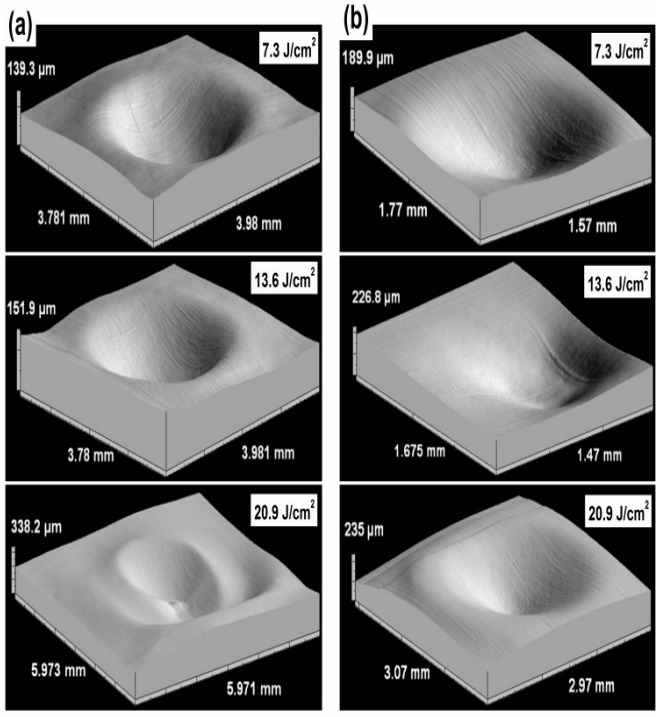

Fig. 7. Surface topography of the craters formed by FPLSF with (a) Glass confinement (b) Water confinement

C. EFFECT OF CONFINEMENT THICKNESS

The effect of confinement layer thickness was analyzed at the following conditions: confinement medium = water, laser fluence = 7.3 J/cm^2 and 13.6 J/cm^2, number of pulses = 1, confinement thickness = 4 mm, 6 mm, and 7 mm. It is observed from Fig. 8 that the crater depth increased from 185 µm to 273 µm while increasing the confinement thickness from 4 mm to 7 mm at 7.3 J/cm^2. When the confinement thickness increases, the laser energy reaching the ablative overlay surface is reduced. This could cause the reduction in the shockwave pressure and hence in the deformation depth. Nevertheless, the increase in plasma pressure was observed with an increase in water layer thickness [10]. This increase in plasma pressure could be responsible for the increase in crater depth with the increase in confinement thickness in this study. However, at 13.6 J/cm^2 fluence, crater depth increased initially and then decreased after reaching a threshold of water thickness (6 mm). This reduction could be attributed to the possible dielectric breakdown of water at higher confinement thickness and at higher laser fluence [6, 10].

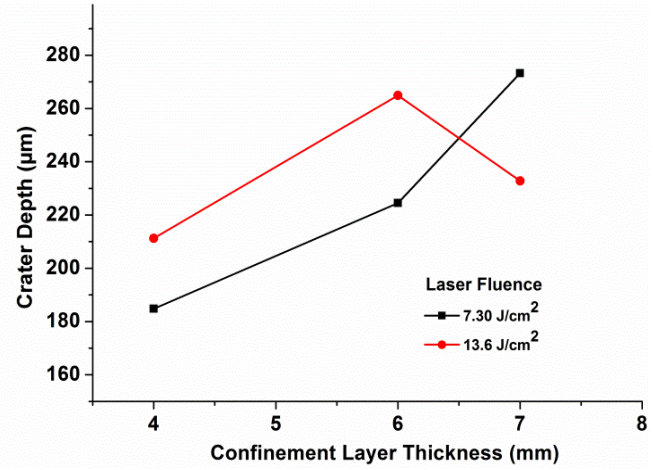

Fig. 8. Effect of confinement layer thickness on the crater depth

D. EFFECT OF NUMBER OF PULSES

The number of laser pulses was examined at the following conditions: laser fluence = 7.3 J/cm^2, 13.6 J/cm^2, and 20.9 J/cm^2; number of pulses = 1, 2, 3 and 10; water confinement thickness = 4 mm. The crater depth is plotted against the number of laser pulses in Fig. 9 for three different laser fluences. It is observed from Fig. 9 that the increase in crater depth was small (0.4%-0.7%) when increasing the number of pulses from 1 to 3 at lower laser fluence levels (7.3 J/cm^2 and 13.6 J/cm^2). It can be concluded that the first pulse accounted for most of the plastic deformation and formed a complete crater. However, only a thin layer of the ablative overlay was vaporized during the first pulse. At second and third pulses, the remaining ablative overlay was vaporized and produced shockwaves which causes further deformation of the craters. The smaller increase in deformation depth in this process can be attributed to the work hardening of the plastically deformed foils. As the yield stress of the formed copper foil increases after the first pulse, further deformation at subsequent pulses is limited. However, a large increase in crater depth (19%) was observed at 20.9 J/cm^2 which is due to the

higher shock pressure generated at 20.9 J/cm^2 fluence.

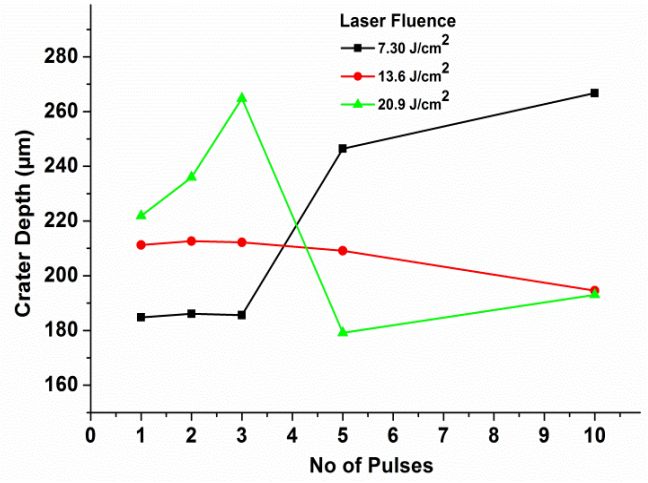

Fig. 9. Effect of number of pulses on the crater depth at different laser fluence

At 10 laser pulses, the crater depth increased by 44% compared to the first pulse crater depth for 7.3 J/cm^2 fluence whereas it decreased drastically for 13.6 J/cm^2 and 20.9 J/cm^2 due to complete ablation of ablative overlay at higher fluence levels.

CONCLUSIONS

The process parameters of FPLSF such as the pad thickness, confinement layer medium, confinement thickness and the number of laser pulses were investigated against the deformation of copper foils in this paper. The following conclusions were obtained based on the results:

(a) The crater depth and diameter increases with increase flexible-pad thickness until a threshold which then reaches saturation.

(b) A significant difference between the crater shapes was observed while using water and glass confinements. Hemispherical craters were formed on the copper foils when using the water confinement whereas shockwave ripples were produced at higher laser fluence when using the glass confinement.

(c) For increase in water confinement thickness from 4 mm to 7 mm, crater depth increased by 48% at 7.3 J/cm^2 whereas decrease in crater depth was observed after the threshold thickness of 6 mm at 13.6 J/cm^2.

(d) It is found that the number of laser pulses is a significant process parameter as there is an optimum number of pulses to achieve the maximum deformation for each laser fluence. It is found that increasing the number of pulses from 1 to 3 resulted only in a small increase (less than 1%) in crater depth at 7.3 J/cm^2 and 13.6 J/cm^2 laser fluence whereas 19.3% increase in depth was observed at 20.9 J/cm^2 laser fluence.

It is understood that the flexible-pad affects the deformation characteristics of FPLSF significantly. Although the pad thickness was analyzed in this paper, the influence of flexible-pad mechanical properties on the deformation behavior of FPLSF needs to be studied further.

ACKNOWLEDGEMENT

This work is supported by Machining Technology Group, Singapore Institute of Manufacturing Technology under CRP Project Number U11-M-013U.

REFERENCES

[1] B. Nagarajan *et al.*, "Mold-free fabrication of 3D microfeatures using laser-induced shock pressure," *Appl. Surf. Sci.,* 2013; 268: 529-534.

[2] F. Vollertsen *et al.*, "On the acting pressure in laser deep drawing," *Production Engineering,* 2009; 3: 1-8.

[3] R. Fabbro *et al.*, "Physics and applications of laser-shock processing," *J. Laser Appl.,* 1998; 10: 265-279.

[4] H. Liu *et al.*, "Micromould based laser shock embossing of thin metal sheets for MEMS applications," *Appl. Surf. Sci.,* 2010; 256: 4687-4691.

[5] X. Hong *et al.*, "Confining medium and absorptive overlay: Their effects on a laser-induced shock wave," *Opt. Lasers Eng.,* 1998; 29: 447-455.

[6] R. Fabbro *et al.*, "Physical study of laser-produced plasma in confined geometry," *J. Appl. Phys.,* 1990; 68: 775-784.

[7] M. Morales *et al.*, "Effect of plasma confinement on laser shock microforming of thin metal sheets," *Appl. Surf. Sci.,* 2011; 257: 5408-5412.

[8] N.B. Dahotre *et al.*, "Laser Shock Processing," *Laser Fabrication and Machining of Materials*, Springer US: 2008, 477-498.

[9] J.P. Romain *et al.*, "Shock waves and acceleration of thin foils by laser pulses in confined plasma interaction," *J. Appl. Phys.,* 1990; 68: 1926-1928.

[10] J.L. Ocana *et al.*, "Laser Shock Processing of Metallic Materials: Coupling of Laser-Plasma Interaction and Material Behaviour Models for the Assessment of Key Process Issues," *AIP Conf. Proc.,* 2010; 1278: 902-913.

[11] C.S. Montross *et al.*, "The influence of coatings on subsurface mechanical properties of laser peened 2011-T3 aluminum," *J. Mater. Sci.,* 2001; 36: 1801-1807.

[12] C. Carey *et al.*, "Effects of Laser Interaction with Graphite Coatings," *Laser Assisted Net Shape Engineering 5, Lane 2007*: 2007, 673-686.

[13] M. Ramezani *et al.*, "Sheet metal forming with the aid of flexible punch, numerical approach and experimental validation," *CIRP Journal of Manufacturing Science and Technology,* 2010; 3: 196-203.

[14] Y. Liu *et al.*, "Studies of the deformation styles of the rubber-pad forming process used for manufacturing metallic bipolar plates," *J. Power Sources,* 2010; 195: 8177-8184.

[15] S.S. Lim *et al.*, "Fabrication of aluminum 1050 micro-channel proton exchange membrane fuel cell bipolar plate using rubber-pad-forming process," *Int. J. Adv. Manuf. Technol.,* 2013; 65: 231-238.

[16] M. Ramezani *et al.*, "Analysis of deep drawing of sheet metal using the Marform process," *Int. J. Adv. Manuf. Technol.,* 2012; 59: 491-505.

[17] S. Thiruvarudchelvan, "Elastomers in metal forming: A review," *J. Mater. Process. Technol.,* 1993; 39: 55-82.